Letter

Direct observation of intrinsic surface magnetic disorder in amorphous superconducting films

Idan Tamir,[1,*] Martina Trahms,[1] Franzisca Gorniaczyk,[2] Felix von Oppen,[3] Dan Shahar,[2] and Katharina J. Franke[1]
[1]*Fachbereich Physik, Freie Universität Berlin, 14195 Berlin, Germany*
[2]*Department of Condensed Matter Physics, The Weizmann Institute of Science, Rehovot 76100, Israel*
[3]*Dahlem Center for Complex Quantum Systems and Fachbereich Physik, Freie Universität Berlin, 14195 Berlin, Germany*

(Received 13 October 2021; revised 26 January 2022; accepted 28 March 2022; published 11 April 2022)

The interplay between disorder and interactions can dramatically influence the physical properties of thin-film superconductors. In the most extreme case, strong disorder is able to suppress superconductivity as an insulating phase emerges. Due to the known pair-breaking potential of magnetic disorder on superconductors, the research focus is on the influence of nonmagnetic disorder. Here we provide direct evidence that magnetic disorder is also present at the surface of amorphous superconducting films. This magnetic disorder is present even in the absence of magnetic impurity atoms and is intimately related to the surface termination itself. While bulk superconductivity survives in sufficiently thick films, we suggest that magnetic disorder may crucially affect the superconductor-to-insulator transition in the thin-film limit.

DOI: 10.1103/PhysRevB.105.L140505

Disorder in superconducting thin films plays a decisive role in the determination of their physical properties. Although Anderson's theorem states that superconductivity is robust with respect to nonmagnetic disorder [1], higher disorder, coupled with the ensuing enhancement of electron-electron interactions, does lead to an eventual reduction in the superfluid density and to local variations of the superconducting order parameter (Δ) [2–4]. Only at very strong disorder superconductivity breaks down and an insulating phase emerges at the superconductor-insulator transition (SIT) [5–8].

In contrast, magnetic disorder has a much stronger impact on superconductivity. This comes about because magnetic scatterers break the time-reversal symmetry necessary for efficient superconducting pairing. As a result, even weak magnetic disorder is expected to lead to strong suppression of superconductivity [9–11]. The possible presence of large amounts of magnetic disorder is thus commonly disregarded when investigating disordered superconductors. Yet, a growing number of experimental observations indicate the presence of intrinsic magnetic surface disorder in various superconductors [12–15].

Direct evidence of magnetic surface disorder may be obtained by scanning tunneling microscopy (STM) and spectroscopy (STS) [16,17]. Magnetic impurities exchange coupled to a superconductor are expected to result in Yu-Shiba-Rusinov (YSR) resonances inside the superconducting energy gap termed YSR states [18–20]. So far, STS has been applied to a number of disordered superconductors [4,21–27]. Most of these studies, using normal-metallic tips, reported on spatial variations in the width of the superconducting energy gap. Yet, YSR states have only been reported for oxygen-rich granular Al (grAl) films and were ascribed to unpaired spins due to the nonstoichiometric composition of the AlO_x layers between the pure Al grains [14].

Here, we use superconducting tips to spatially resolve variations in the spectra of the superconducting energy gap at the surface of amorphous indium oxide (a:InO) films, a frequently studied disordered superconductor [5,28]. Our results are obtained from six different superconducting a:InO films, grown *ex situ*, with different degrees of disorder (for sample preparation and transport characterization see Supplemental Material (SM) [29]). The films have relatively high critical temperatures [30], $T_C \gtrsim 2.5$ K (well above our base temperature, $T = 1$–1.3 K), as confirmed prior to the STM experiments by transport measurements (see SM for more details [29]).

We observe an abundance of subgap peaks on the surface of the a:InO films. In fact, if we also consider asymmetry in the height of the coherence peaks as an indication of weakly bound subgap peaks [31,32], we hardly observe any spectra that follow the classic predictions of the Bardeen-Cooper-Schrieffer (BCS) theory [33]. The response of these peaks to high-frequency radiation and tip approach suggests that these are YSR states [34–37], and, although some experiments indicate the existence of surface magnetic disorder in similar systems [38–40], our results present, to the best of our knowledge, the first direct evidence. We also show that the presence of magnetic scattering centers is not due to surface contamination and argue that it stems from the intrinsic presence of unsaturated bonds at the surface. Finally, while surface magnetic disorder should not suppress superconductivity in the bulk of the materials, we suggest that the role of surface magnetism will substantially increase when approaching the thin-film limit [41,42]. The SIT may well be affected by the presence of surface magnetic disorder at this stage.

Our observations are made possible by utilizing superconducting tips (lead or niobium), shaped and characterized in ultrahigh vacuum to achieve atomic-scale spatial

*Idan.Tamir@FU-Berlin.de

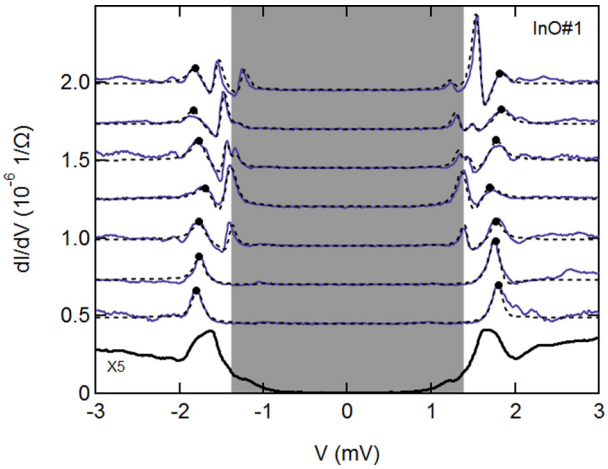

FIG. 1. Observation of subgap states. Representative local dI/dV vs. V spectra (blue) observed by STS of an a:InO film. Traces are vertically shifted for visibility. The gray shaded region indicates $eV \leqslant \Delta_{\text{tip}}$. Data are measured at $T = 1.3$ K, and feedback opened at $I = 200$ pA and $V = 4$ mV, lock-in amplitude is 15 μV. The dashed black lines are fits to the data using a phenomenological model to include the effect of YSR states (for details see SM [29]). Black circles indicate the coherence-peak positions from the fits. The bottom-most trace (black, multiplied by five for visibility) is the average of all 400 evenly spaced spectra measured within a 100×100 nm^2 scan range from which the representative spectra were selected.

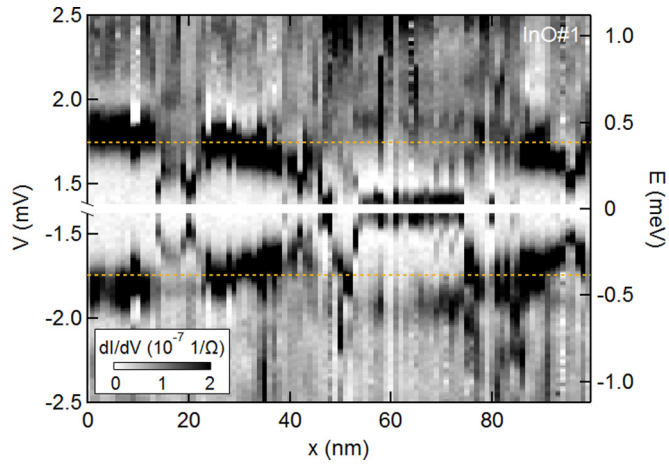

FIG. 2. Spatial variations. Grayscale map of dI/dV spectra measured along a line. The orange dashed lines indicate the averaged energy gap of the a:InO film. Data at energies smaller than the superconducting energy gap of the tip ($eV \leqslant \Delta_{\text{tip}} = 1.38$ meV) are omitted for clarity, full spectral range is shown in SM [29]. Data are measured at $T = 1.3$ K, and feedback opened at $I = 130$ pA and $V = 2.5$ mV, lock-in amplitude is 15 μV. We note that the presence of a subgap excitation reduces the amplitude of the coherence peak.

resolution. By using superconducting tips we overcome the thermal broadening limit ($\sim 3.5\, k_B T \approx 0.3$ meV at $T = 1$ K, where k_B is the Boltzmann constant), usually governing the energy resolution of spectroscopic measurements, and greatly improve the signal to noise ratio with respect to normal-metallic tips. The measured spectra are then a convolution of sample and tip densities of states (DoSs) rather than being directly proportional to the sample's DoS. As a result, all of the sample related spectroscopic features are shifted in voltage (V) by the superconducting gap of the tip [43] ($\Delta_{\text{tip}}/e = 1.3$–$1.5$ mV, where e is the electron charge, see SM for more details [29]).

To survey the local superconducting properties, we record differential conductance (dI/dV) spectra on several macroscopically separated surface areas. Representative high-resolution spectra measured at different positions within one of these areas, in a range of 100×100 nm^2, are presented in Fig. 1 (data collected on other samples is available in the SM [29]). Notably, most of the data do not resemble conventional BCS spectra. Instead, we often observe several peaks, symmetric in voltage, but asymmetric in intensity, and at varying subgap energies. The specific ratio of conventional BCS spectra to those exhibiting subgap peaks is sample and position dependent. For example, the data used in Fig. 1 are selected from 400 evenly spaced spectra, all measured within the same scan range, about 60% of which exhibit well-resolved subgap peaks. We are able to capture the spectroscopic details of the data presented in Fig. 1 by superimposing subgap quasiparticle states, at energies $\pm\varepsilon \leqslant \Delta$, to the BCS form used to describe our sample's DoS. The fits to the spectra using this phenomenological model are plotted as black dashed lines in the figure (for full fit equation see SM [29]). Note that peaks inside the tip's gap (gray shaded region in Fig. 1 are related to thermal occupation of quasiparticles [43], see SM [29]).

Next we probe the spatial extent of the subgap peaks. To do so we record densely (1 nm) spaced spectra along lines across the surface. An example is shown in Fig. 2. We find a variety of subgap peaks at different energies, ranging from deep inside the a:InO superconducting energy gap to its edge, which is indicated by the dashed orange lines (for clarity, we left out data at energies smaller than Δ_{tip}, the complete spectra are available in the SM [29]). While some of the subgap peaks are rather local, others spread over a few nanometers.

The abrupt changes between the closely spaced spectra indicate a fast decay of the subgap states, related to the three-dimensional nature of the electronic system [16,44], and are clear evidence for the need for highly resolved data. We further emphasize the importance of high spatial resolution by including in Fig. 1 the average of the entire set of spectra taken on the equidistant grid from which the representative data of that figure were selected (black, amplitude times five). The average's shape may easily be interpreted as a signature of BCS superconductivity with an unexplained, but not uncommon [4,8,22–24,45], nonvanishing subgap conductivity. Comparison to the highly resolved local data shows that this averaging obscures the details of the subgap structure and, thus, may lead to different conclusions on the superconducting properties.

To gain further insight into the nature of the subgap states, we explore the influence of the STM tip on their excitation energy. Increasing the tunnel junction conductance by approaching with the STM tip toward the surface can result in an increase in the energy, ε, of the subgap states, as seen in Figs. 3(a), 3(b). At even higher conductances, ε saturates at the energy of the coherence peaks. Similar observations are made in other systems, where the subgap peaks are attributed to YSR states [34–36]. Two possible mechanisms are

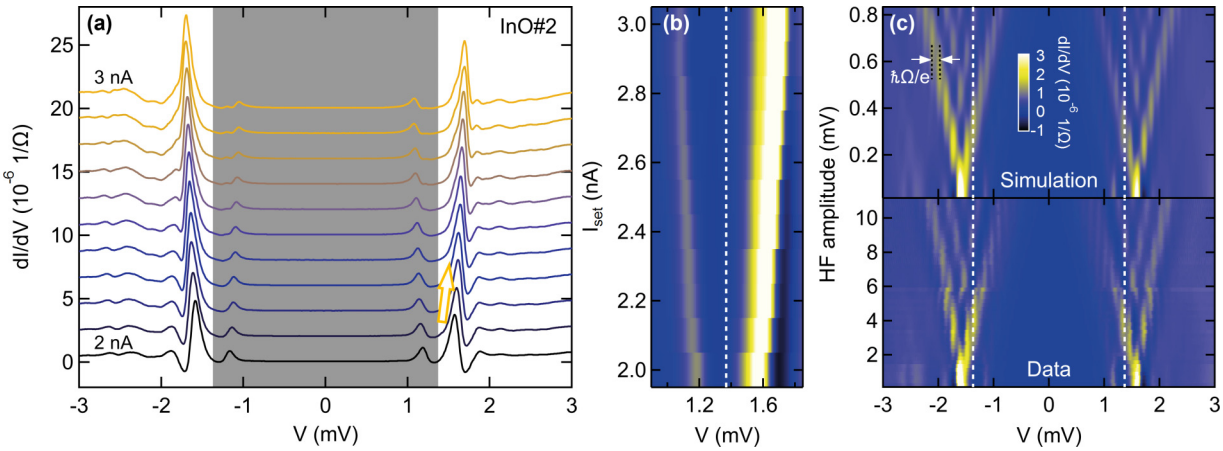

FIG. 3. Approaching the surface and response to HF. (a) dI/dV vs. V measured at different set currents from 2 nA (black) to 3 nA (orange) using 0.1 nA steps. The energy of the YSR state initially at $|\varepsilon + \Delta_{\text{tip}}| \sim 1.5$ mV is shifted towards the coherence peaks that are initially barely resolved. The subgap peak's energy trend is indicated by the arrow. Spectra are vertically shifted for visibility. The gray shaded region indicates $eV \leqslant \Delta_{\text{tip}}$. Data are measured at $T = 1.3$ K, feedback is opened at $V = 4$ mV, lock-in amplitude is 15 μV. (b) Color-scale map of spectra using the same data as in (a). For color scale, see (c). Map focuses on positive V for better visibility. Dashed line indicates Δ_{tip}. The enhanced conductance below Δ_{tip}/e is related to the thermal replica of the $V < 0$ YSR state. (c) Color-scale map of dI/dV spectra measured at different HF power, bottom, and simulation assuming that single-electron tunneling dominates the transport ($\hbar\Omega/e$ splitting), top. Dashed lines indicate Δ_{tip}. Data are measured at the same position, as in (a), with the feedback opened at $V = 4$ mV and $I = 2$ nA. Differences in the HF amplitudes between measurement and simulation stem from damping in our transmission line.

suggested: First, pulling or pushing of a magnetic impurity due to van der Waals forces between tip and impurity, which in turn change the coupling between the magnetic impurity and the superconducting substrate [34,35]. Second, local gating by the tip, which changes the electrostatic background [36]. Due to the low tunnel-junction conductance used and the low charge density in our samples [5], we favor the latter explanation. Importantly, both explanations are compatible with a YSR origin of the observed subgap states.

We note that the observed subgap states are not consistent with the recently reported collective gap in highly disordered superconducting a:InO films [46]. In their report, Dubouchet *et al.* observe subgap peaks that appear at high tunnel-junction transmission, larger than the conductance quantum ($G_0 = 2e^2/h$), and associate them with tunneling processes involving two electrons that indicate a collective energy gap of preformed Cooper pairs. Our samples, however, are far from the SIT, and our measurements are conducted in the low transmission limit. Furthermore, while only tunneling processes involving two electrons are relevant to the observation of a collective gap, we are able to determine the single-particle nature of electrons tunneling into the subgap states we report here. This is done by irradiating the tunnel junction by high-frequency radiation [(HF) $\nu = 30$ GHz]. Introducing radiation results in photon-assisted tunneling such that zero-radiation power conductance peaks split in energy into several peaks with a separation inversely proportional to the excitation's charge ke, $\delta V = h\nu/ke$, where h is Planck's constant and k is an integer [37,47–50].

A color-coded set of spectra with increasing HF amplitude is shown in Fig. 3(c), bottom panel. The pronounced subgap peaks are seen in white at the bottom of the map (lowest HF power). As we increase the HF power a splitting of the peaks is observed. Following Ref. [37] we simulated the data using only the spectrum measured without HF radiation and ν as input parameters. We find excellent agreement between experiment and the single-particle simulation ($k = 1$).

A similar behavior of the subgap states in response to HF radiation and upon tip approach has been observed for YSR states [34–37], supporting this interpretation. However, Andreev bound states could potentially respond in a similar way [51]. These might arise in regions where the superconducting gap is locally much reduced, confining electrons by Andreev reflections occurring at the boundaries. These bound states would also induce similar peaks in the measured dI/dV appearing symmetrically around the Fermi energy inside of the superconducting gap. However, our observation of states deep inside the superconducting energy gap would require a dramatic reduction of the superconducting gap in large parts of the surface. This is at odds with our fits of the data and with previously reported gap variations of 10–20 % in moderately disordered films [4,24,27]. Hence, we find this scenario unlikely and favor the interpretation in terms of YSR states. The occurrence of local subgap states (demonstrated in Fig. 2, and also in the SM) further supports this conclusion. If the origin of these states were some other variation of the superconducting order parameter, one would have expected them to vary on the length scale of the coherence length (estimated to be 4–5 nm [30]). This is not the case. Finally, based on the number of spectra exhibiting subgap states, we can give an upper bound of $\leqslant$60% of the surface area affected by magnetic impurities (for example, see data in Fig. 1).

Having established the observation of spatially varying YSR states, we now discuss their magnetic origin. One may suspect that the YSR states are due to magnetic impurities arising from surface modifications induced, e.g., by surface oxide formation, or any other impurity absorption during storage. We took measures to remove several surface

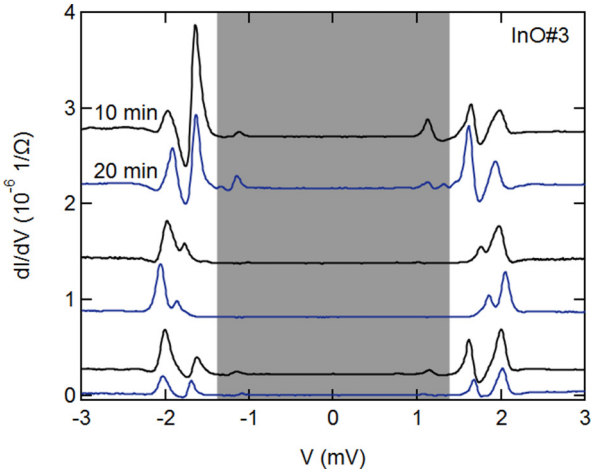

FIG. 4. Removing surface layers. Characteristic spectra, shifted for visibility, exhibiting pronounced YSR states. The spectra are measured after the first (black), and second sputtering cycle (blue). Data are measured at $T = 1.3$ K, and feedback opened at $I = 200$ pA and $V = 4$ mV, lock-in amplitude is 15 μV. The gray shaded region indicates eV $\leqslant \Delta_{\text{tip}}$.

layers by sputtering. We set the sputtering parameters to remove approximately a 1 Å thick layer of surface atoms per minute, and conducted two sputtering cycles, 10 min each. For this experiment we used a thick sample (300 nm) to avoid thickness-dependent effects.

Post sputtering, we do not detect any qualitative change. In Fig. 4 we present spectra exhibiting similar YSR states after the first (black), and second sputtering cycle (blue). The spectra are shifted vertically for visibility. While we choose to present prominent subgap features, the entire sets of data acquired after sputtering are qualitatively very similar to each other and to data collected on other films without sputtering. Even after two sputtering cycles, the majority of individual spectra exhibit YSR states. If this finding was representing bulk properties, this would be very surprising. This would imply an extremely high density of magnetic impurities, which are expected to strongly suppress superconductivity [9–11]. If, in contrast, the magnetic impurities are limited to the surface, superconductivity in the bulk would be hardly affected. Given the persistent superconducting state, we interpret the occurrence of YSR states as a surface effect. The termination of the sample inevitably exposes unsaturated bonds, which involve unpaired electrons giving rise to YSR states. Each sputtering cycle exposes new material, yet always exhibiting unsaturated bonds. We therefore conclude that the surface magnetic disorder is intrinsic.

We emphasize that, in contrast to Ref. [14], the YSR states in our films are limited to the surface. Nonetheless, we believe that magnetic surface disorder due to unsaturated bonds may be generic to oxygen-rich materials and should be considered as additional parameter in the complexity of disordered superconducting films. Most prominently, surface effects may play a significant role in thin samples. We speculate that the SIT in such systems could be affected by the enhanced exchange scattering at the surface. Specifically, local breaking of time-reversal symmetry due to magnetic impurities could reduce the overall phase coherence, which would in turn affect Cooper-pair localization [21,52,53] close to the SIT.

We also expect the presence of surface magnetic disorder to result in a finite contribution to the real part of the optical conductivity at subgap energies (σ_1, measured via electromagnetic absorption). This follows from measurements of quenched superconducting films containing magnetic impurities [54]. Recently, finite subgap conductivity (σ_1) measured in moderately disordered a:InO films was explained in terms of the Higgs mechanism [55]. Considering our findings, one would need to take into account a parallel contribution to σ_1, originating from the unavoidable surface magnetic disorder, when estimating the magnitude of the Higgs contribution.

In conclusion, using superconducting STM tips, we have identified a large abundance of subgap states on the surface of a:InO. Their response to high-frequency radiation as well as to the proximity of the STM tip suggests that they are of magnetic origin. Though sputtering does not affect the occurrence of the YSR states, they are most likely a surface-related phenomenon as superconductivity could not persist with such a large density of magnetic impurities in the bulk. We suggest that dangling bonds at the sample's termination provide the unpaired electron spins. One may then consider strategies in tuning the number of unsaturated bonds by annealing in vacuum or controlled oxygen exposure. Simultaneously tracking the SIT may further shed light on the role of magnetic disorder on the SIT.

We acknowledge financial support by Deutsche Forschungsgemeinschaft through Grant CRC 183 (Project No. C03) and JOSPEC (FR-2726/5). This research was supported by Grant No 2018024 from the United States-Israel Binational Science Foundation (BSF). I.T. acknowledges funding from the Alexander-von-Humboldt foundation in the framework of Humboldt Research Fellowship for Postdoctoral Researchers, and from the DFG in the framework of the Walter Benjamin Position (Grant No. TA 1722/1-1).

[1] P. Anderson, J. Phys. Chem. Solids **11**, 26 (1959).
[2] A. Larkin and Y. N. Ovchinnikov, Zh. Eksp. Teor. Fiz. **61**, 1221 (1971) [Sov. Phys. JETP **34**, 651 (1972)].
[3] M. Ma and P. A. Lee, Phys. Rev. B **32**, 5658 (1985).
[4] B. Sacépé, C. Chapelier, T. I. Baturina, V. M. Vinokur, M. R. Baklanov, and M. Sanquer, Phys. Rev. Lett. **101**, 157006 (2008).
[5] D. Shahar and Z. Ovadyahu, Phys. Rev. B **46**, 10917 (1992).
[6] A. M. Goldman and N. Markovic, Phys. Today **51**(11), 39 (1998).
[7] V. F. Gantmakher and V. T. Dolgopolov, Phys. Usp. **53**, 1 (2010).
[8] B. Sacépé, M. Feigel'man, and T. M. Klapwijk, Nat. Phys. **16**, 734 (2020).

[9] A. A. Abrikosov and L. P. Gor'kov, Zh. Eksp. Teor. Fiz. **39**, 480 (1960) [Sov. Phys. JETP **12**, 337 (1961)].

[10] J. K. Tsang and D. M. Ginsberg, Phys. Rev. B **21**, 132 (1980).

[11] J. A. Chervenak and J. M. Valles, Phys. Rev. B **51**, 11977 (1995).

[12] S. Sendelbach, D. Hover, A. Kittel, M. Mück, J. M. Martinis, and R. McDermott, Phys. Rev. Lett. **100**, 227006 (2008).

[13] N. A. Saveskul, N. A. Titova, E. M. Baeva, A. V. Semenov, A. V. Lubenchenko, S. Saha, H. Reddy, S. I. Bogdanov, E. E. Marinero, V. M. Shalaev, A. Boltasseva, V. S. Khrapai, A. I. Kardakova, and G. N. Goltsman, Phys. Rev. Applied **12**, 054001 (2019).

[14] F. Yang, T. Gozlinski, T. Storbeck, L. Grünhaupt, I. M. Pop, and W. Wulfhekel, Phys. Rev. B **102**, 104502 (2020).

[15] G. Zhang, T. Samuely, N. Iwahara, J. Kačmarčík, C. Wang, P. W. May, J. K. Jochum, O. Onufriienko, P. Szabó, S. Zhou *et al.*, Sci. Adv. **6**, eaaz2536 (2020).

[16] A. Yazdani, B. A. Jones, C. P. Lutz, M. F. Crommie, and D. M. Eigler, Science **275**, 1767 (1997).

[17] B. W. Heinrich, J. I. Pascual, and K. J. Franke, Prog. Surf. Sci. **93**, 1 (2018).

[18] L. Yu, Acta Phys. Sin **21**, 75 (1965).

[19] H. Shiba, Prog. Theor. Phys. **40**, 435 (1968).

[20] A. Rusinov, JETP Lett. **9**, 85 (1969).

[21] B. Sacépé, T. Dubouchet, C. Chapelier, M. Sanquer, M. Ovadia, D. Shahar, M. Feigel'man, and L. Ioffe, Nat. Phys. **7**, 239 (2011).

[22] M. Chand, G. Saraswat, A. Kamlapure, M. Mondal, S. Kumar, J. Jesudasan, V. Bagwe, L. Benfatto, V. Tripathi, and P. Raychaudhuri, Phys. Rev. B **85**, 014508 (2012).

[23] Y. Noat, V. Cherkez, C. Brun, T. Cren, C. Carbillet, F. Debontridder, K. Ilin, M. Siegel, A. Semenov, H.-W. Hübers, and D. Roditchev, Phys. Rev. B **88**, 014503 (2013).

[24] P. Szabó, T. Samuely, V. Hašková, J. Kačmarčík, M. Žemlička, M. Grajcar, J. G. Rodrigo, and P. Samuely, Phys. Rev. B **93**, 014505 (2016).

[25] D. Lotnyk, O. Onufriienko, T. Samuely, O. Shylenko, V. Komanický, P. Szabó, A. Feher, and P. Samuely, Low Temp. Phys. **43**, 919 (2017).

[26] W.-T. Liao, T. P. Kohler, K. D. Osborn, R. E. Butera, C. J. Lobb, F. C. Wellstood, and M. Dreyer, Phys. Rev. B **100**, 214505 (2019).

[27] C. Carbillet, V. Cherkez, M. A. Skvortsov, M. V. Feigel'man, F. Debontridder, L. B. Ioffe, V. S. Stolyarov, K. Ilin, M. Siegel, D. Roditchev, T. Cren, and C. Brun, Phys. Rev. B **102**, 024504 (2020).

[28] A. F. Hebard and M. A. Paalanen, Phys. Rev. Lett. **65**, 927 (1990).

[29] See Supplemental Material at http://link.aps.org/supplemental/10.1103/PhysRevB.105.L140505 for samples details, further information regarding the use of superconducting tips, and details regarding the phenomenological model used in the main text.

[30] B. Sacépé, J. Seidemann, M. Ovadia, I. Tamir, D. Shahar, C. Chapelier, C. Strunk, and B. A. Piot, Phys. Rev. B **91**, 220508(R) (2015).

[31] J. Homberg, A. Weismann, R. Berndt, and M. Gruber, ACS Nano **14**, 17387 (2020).

[32] A. Odobesko, D. Di Sante, A. Kowalski, S. Wilfert, F. Friedrich, R. Thomale, G. Sangiovanni, and M. Bode, Phys. Rev. B **102**, 174504 (2020).

[33] J. Bardeen, L. N. Cooper, and J. R. Schrieffer, Phys. Rev. **108**, 1175 (1957).

[34] L. Farinacci, G. Ahmadi, G. Reecht, M. Ruby, N. Bogdanoff, O. Peters, B. W. Heinrich, F. von Oppen, and K. J. Franke, Phys. Rev. Lett. **121**, 196803 (2018).

[35] H. Huang, R. Drost, J. Senkpiel, C. Padurariu, B. Kubala, A. L. Yeyati, J. C. Cuevas, J. Ankerhold, K. Kern, and C. R. Ast, Commun. Phys. **3**, 199 (2020).

[36] D. Chatzopoulos, D. Cho, K. M. Bastiaans, G. O. Steffensen, D. Bouwmeester, A. Akbari, G. Gu, J. Paaske, B. M. Andersen, and M. P. Allan, Nat. Commun. **12**, 298 (2021).

[37] O. Peters, N. Bogdanoff, S. A. González, L. Melischek, J. R. Simon, G. Reecht, C. B. Winkelmann, F. von Oppen, and K. J. Franke, Nat. Phys. **16**, 1222 (2020).

[38] N. H. Hong, J. Sakai, N. Poirot, and V. Brizé, Phys. Rev. B **73**, 132404 (2006).

[39] S. E. de Graaf, A. A. Adamyan, T. Lindström, D. Erts, S. E. Kubatkin, A. Y. Tzalenchuk, and A. V. Danilov, Phys. Rev. Lett. **118**, 057703 (2017).

[40] S. Mumford, T. Paul, and A. Kapitulnik, Phys. Rev. Materials **5**, 125201 (2021).

[41] D. B. Haviland, Y. Liu, and A. M. Goldman, Phys. Rev. Lett. **62**, 2180 (1989).

[42] V. Hašková, M. Kopčík, P. Szabó, T. Samuely, J. Kačmarčík, O. Onufriienko, M. Žemlička, P. Neilinger, M. Grajcar, and P. Samuely, Appl. Surf. Sci. **461**, 143 (2018).

[43] M. Ruby, F. Pientka, Y. Peng, F. von Oppen, B. W. Heinrich, and K. J. Franke, Phys. Rev. Lett. **115**, 087001 (2015).

[44] G. C. Ménard, S. Guissart, C. Brun, S. Pons, V. S. Stolyarov, F. Debontridder, M. V. Leclerc, E. Janod, L. Cario, D. Roditchev *et al.*, Nat. Phys. **11**, 1013 (2015).

[45] F. Herman and R. Hlubina, Phys. Rev. B **94**, 144508 (2016).

[46] T. Dubouchet, B. Sacépé, J. Seidemann, D. Shahar, M. Sanquer, and C. Chapelier, Nat. Phys. **15**, 233 (2019).

[47] P. K. Tien and J. P. Gordon, Phys. Rev. **129**, 647 (1963).

[48] A. Roychowdhury, M. Dreyer, J. R. Anderson, C. J. Lobb, and F. C. Wellstood, Phys. Rev. Applied **4**, 034011 (2015).

[49] P. Kot, R. Drost, M. Uhl, J. Ankerhold, J. C. Cuevas, and C. R. Ast, Phys. Rev. B **101**, 134507 (2020).

[50] S. A. González, L. Melischek, O. Peters, K. Flensberg, K. J. Franke, and F. von Oppen, Phys. Rev. B **102**, 045413 (2020).

[51] J. A. Sauls, Phil. Trans. R. Soc. A. **376**, 20180140 (2018).

[52] M. V. Feigel'man, L. B. Ioffe, V. E. Kravtsov, and E. A. Yuzbashyan, Phys. Rev. Lett. **98**, 027001 (2007).

[53] M. Feigel'man, L. Ioffe, V. Kravtsov, and E. Cuevas, Ann. Phys. (NY) **325**, 1390 (2010), July 2010 Special Issue.

[54] G. J. Dick and F. Reif, Phys. Rev. **181**, 774 (1969).

[55] D. Sherman, U. S. Pracht, B. Gorshunov, S. Poran, J. Jesudasan, M. Chand, P. Raychaudhuri, M. Swanson, N. Trivedi, A. Auerbach *et al.*, Nat. Phys. **11**, 188 (2015).